DOI 10.1007/s10778-023-01181-6
International Applied Mechanics, Vol. 58, No. 5, September, 2022

NONLINEAR DEFORMATION OF DISCRETELY INHOMOGENEOUS SHALLOW SHELLS BASED ON THE GENERALIZED METHOD OF FINITE INTEGRAL TRANSFORMS*

O. I. Bespalova

A numerical analytical approach to the study of the nonlinear deformation of shallow shells under subcritical loads is proposed. The approach rationally combines the generalized method of finite integral transforms and the Newton–Kantorovich–Raphson linearization method. The static stiffness and load–deflection relationship of flexible shallow shells with various boundary conditions in a wide range of changes in their Gaussian curvature and the presence of discrete inclusions are analyzed. It is shown that the dependence of the upper critical values of external pressure on the location of discrete inclusions is nonmonotonic, which makes it possible to determine their optimal location in terms of the static stability and bearing capacity of the shells.

Keywords: shallow shells, discrete inclusions, static stability, generalized method of finite integral transforms, quasilinearization method, analysis

Introduction. Shallow shells cover a wide class of thin-walled objects used as structural members in mechanical engineering, construction, aerospace, and marine engineering, etc., and are described by certain features of their mechanical behavior. The analysis of their stationary strain, including the stress–strain state, vibrations, and stability under various types of static loads is an important condition for assessing the functional suitability of these shells in real operating condition.

Studying the nonlinear deformation of shallow shells in its various aspects, including static stability, is still of interest [15, 17, 24].

Scientific and technical projects focused on solving specific practical problems and are in demand in terms of architectural evaluation of modern design have become widespread. Thus, the project [19] solved the problem of geometrically nonlinear behavior of shells using, as an example, a real gymnasium roof in Halstenbek (Weimar, Germany) that collapsed twice by losing stability during construction. The steel and glass roof was designed as a shallow shell with an oval planform, the critical values of wind load and external pressure were determined, the effect of supports, joints, etc. was determined using the finite-element method (FEM, ANSYS).

The use of shallow panels in traditional and mechanized mining methods, the determination of maximum safe spans, rational orientation of connecting elements in dome structures are addressed in [21, 24].

Fundamental research on this topic covers inhomogeneous shells of complex structure across thickness: multilayer (discretely inhomogeneous) shells and shells made of functional gradient (continuously inhomogeneous) materials [8, 9, 14, 15, 18, 23]. As a means of increasing the bearing capacity of elastic objects, isotropic and orthotropic shallow shells of variable thickness in one [1] and two [17] coordinate directions were considered.

S. P. Timoshenko Institute of Mechanics, National Academy of Sciences of Ukraine, 3 Nesterova St., Kyiv, Ukraine, 03057; e-mail: elena_bespalova@ukr.net. Translated from Prykladna Mekhanika, Vol. 58, No. 5, pp. 81–96, September–October 2022. Original article submitted August 17, 2021.

* This study was sponsored by the budget program “Support for Priority Areas of Scientific Research” (KPKVK 6541230).

The stability of shells in static fields of various nature, including a thermal medium, external pressure and wind, concentrated mechanical compression and localized thermal loads, etc. was analyzed in [6, 13, 14, 18–20, 22, 23, 25].

Studies of the nonlinear deformation of shallow shells and plates made of nanomaterials, as a relevant field of development of solid mechanics intensify [15].

The stability of shallow shells and panels is often analyzed for are hinged, clamped, and combined boundary conditions [6, 9, 25] and quite rarely analyzed for free sections of the unloaded boundary [20], although this type of boundary conditions is quite common in construction.

The mathematical apparatus for solving relevant (non)linear boundary-value problems is represented in most cases by various FEM schemes, the Ritz variational method, the Galerkin projection method in combination with modern refinements of linear and nonlinear algebra [1, 6, 14, 15, 17–19]. Note that nontraditional approaches can be applied to linear problems such as the method of discrete Fourier series [16], the method of complete systems [12].

A separate group of so-called discretely inhomogeneous shells should be distinguished. In such shells, various types of reinforcing elements (ribs, pads, bandages, elastic supports) are used to increase their stiffness and stability. According to technological requirements, they can also have different types of cuts and holes. It is naturally necessary to choose rational geometrical parameters of shells, stiffness characteristics of discrete inclusions, their optimal placement, etc.

This article proposes a new solution to the nonlinear two-dimensional boundary-value problem for determining the stress–strain state (SSS) of shell elements during subcritical deformation based on a combination of the generalized method of finite integral transforms and the Newton–Kantorovich–Raphson linearization method. The developed approach is used to analyze the SSS of flexible shallow panels over a wide range of change in their Gaussian curvature and to analyze the effect of the location of discrete inclusions on the stability of these shells.

1. Problem Statement. Consider a shallow shell of constant thickness h. Its midsurface occupies a rectangular domain $\Omega \cup \partial\Omega = \{x, y: x \in [x_0, x_1],\ y \in [y_0, y_1]\}$ in the projections onto the Cartesian coordinate system x, y, has curvatures k_x, k_y along the coordinate axes and the Gaussian curvature $K = k_x k_y$. The shell is located on an elastic Winkler foundation with coefficient $K_p = K_p(x, y)$, and in the domain Ω. It is under a vector of distributed loads $\vec{q} = \{q_x, q_y, q_n\}$, where n is the normal to its midsurface. No restrictions, except their physical incompatibility, are imposed on the boundary conditions, so that the forces and moments, displacements or their combinations can be specified at each point of the boundary $\partial\Omega$. The shell material is assumed to be isotropic and linearly elastic in the entire range of operating loads up to their critical values.

This class of thin-walled objects includes: rectangular plates ($k_x = 0, k_y = 0, K = 0$), cylindrical panels ($k_x = 0, k_y \neq 0, K = 0$), elements of spherical ($k_x > 0, k_y > 0, K > 0$) and saddle-shaped ($k_x > 0, k_y < 0, K < 0$) shells.

The mechanical-mathematical model of the deformation of such shells under subcritical loads is based on the geometrically nonlinear theory of medium bending of second order according to the Donnell–Mushtari–Vlasov theory and is described by a nonlinear two-dimensional boundary-value problem that can be represented in the following vector-matrix form (see [4]):

$$D(\vec{U}) = L\vec{U} + \vec{g} + \vec{f} = 0, \qquad (x, y) \in \Omega, \tag{1}$$

$$G_{xp}(\vec{U}) = R_{xp}\vec{U} + \vec{s}_{xp} + \vec{\varphi}_{xp} = 0, \qquad x = x_p \quad (p = 0, 1), \tag{2}$$

$$G_{yp}(\vec{U}) = R_{yp}\vec{U} + \vec{s}_{yp} + \vec{\varphi}_{yp} = 0, \qquad y = y_p \quad (p = 0, 1), \tag{3}$$

where $D(\vec{U})$ and $G_{xp}(\vec{U})$, $G_{yp}(\vec{U})$ are nonlinear matrix differential operators given in the domain Ω and on its boundary $\partial\Omega$; $\vec{U} = \{u(x, y), v(x, y), w(x, y)\}$ is an unknown vector function whose components are the displacement u, v, w along the coordinate axes $0x$, $0y$ and along the normal to them; $L = \{l_{ij}\}$ $(i, j = 1, 2, 3)$, $\vec{g} = \{g_i(x, y)\}$ $(i = \overline{1, 3})$ and $\vec{f} = \{f_i(x, y)\}$ $(i = \overline{1, 3})$ $(f_i(x, y) = -q_i(x, y))$ are a matrix linear differential operator, a vector function of nonlinear terms, and the free term defined in the domain Ω; $R_{xp} = \{r_{ij}^{(xp)}\}$ $(i = \overline{1, 3},\ j = \overline{1, 4})$, $\vec{s}_{xp} = \{s_i^{xp}(x, y)\}$ $(i = \overline{1, 4})$ and $\vec{\varphi}_{xp} = \{\varphi_{xp}(x, y)\}$ $(i = \overline{1, 4})$ are a matrix linear differential or algebraic operator, the vector function of nonlinear terms, and the free term in the boundary conditions at the edge $x = x_p$ $(p = 0, 1)$; the operator and vector functions with the index y_p for the boundary conditions at $y = y_p$ $(p = 0, 1)$ have a similar sense.

The expressions for the elements of these operators and components of vector functions are obtained using the standard differentiation method.

2. Numerical Analytical Approach to Solving Nonlinear Two-Dimensional Problems (General Scheme). We propose a numerical analytical approach based on the generalized method of finite integral transforms and the Newton–Kantorovich–Raphson linearization method (quasilinearization method) to solve the nonlinear two-dimensional boundary-value problem (1)–(3).

The quasilinearization method [2] has some advantages over the other linearization methods. This is, in particular, the application domain that coincides with the domain of convexity of the operator of the problem and, as shown in [3], with the subcritical stage of deformation of the shell, quadratic convergence and algorithmicity of the iterative process, ease of selection of the initial approximation, etc.

The generalized method of finite integral transforms (MFIT*) is focused on solving N-dimensional ($N \geq 2$) problems with inseparable variables. For linear problems, its main provisions are stated in [10] (two-dimensional problems of the statics of inhomogeneous plates) and in [11] (three-dimensional problems of the theory of elasticity of anisotropic prisms). The essence of this method in the two-dimensional case is to develop two integral transforms with respect to different domain variables, so that the kernel functions of one transform are transform functions of the other one and vice versa. The unknown kernel functions of the developed transforms are determined from the coupled system of two one-dimensional problems, which is solved by an iterative method analogous to the Liebmann–Gauss–Seidel process in linear algebra. The unknown solution of the original problem is determined using the inverse integral transform found from the kernel functions.

According to the developed approach, the solution of the nonlinear two-dimensional boundary-value problem consists of the following stages.

Reduction of the nonlinear problem to an iterative sequence of linearized boundary-value problems using the quasilinearization method.

Solution of each linearized problem by the MFIT* using two integral transforms with respect to different domain variables.

Development of a joint iterative process that includes the linearization of the original problem and the determination of the kernel functions from the system of two integral transforms.

Stage 1. Application of the quasilinearization method to the original nonlinear problem (1)–(3) reduces it to an iterative sequence of linearized two-dimensional boundary-value problems of the following form ($n = 1, 2, \ldots$ is the linearization parameter):

$$D(\vec{U}^{(n)}, \vec{U}^{(n-1)}, \ldots) = L\vec{U}^{(n)} + J_{,\vec{U}}(\vec{U}^{(n)} - \vec{U}^{(n-1)}) + J_{,\vec{U},x}(\vec{U}_{,x}^{(n)} - \vec{U}_{,x}^{(n-1)})$$

$$+ J_{,\vec{U},xx}(\vec{U}_{,xx}^{(n)} - \vec{U}_{,xx}^{(n-1)}) + J_{,\vec{U},y}(\vec{U}_{,y}^{(n)} - \vec{U}_{,y}^{(n-1)}) + J_{,\vec{U},xy}(\vec{U}_{,xy}^{(n)} - \vec{U}_{,xy}^{(n-1)}) + \ldots$$

$$+ \vec{g}(\vec{U}^{(n-1)}, \vec{U}_{,x}^{(n-1)}, \ldots) + \vec{f} = 0, \quad (x, y) \in \Omega, \tag{4}$$

$$G_{xp}(\vec{U}^{(n)}, \vec{U}^{(n-1)}, \ldots) = R_{xp}\vec{U}^{(n)} + I_{,\vec{U}}(\vec{U}^{(n)} - \vec{U}^{(n-1)}) + I_{,\vec{U},x}(\vec{U}_{,x}^{(n)} - \vec{U}_{,x}^{(n-1)})$$

$$+ I_{,\vec{U},y}(\vec{U}_{,y}^{(n)} - \vec{U}_{,y}^{(n-1)}) + \vec{\varphi}_{xp} = 0, \quad x = x_p \quad (p = 0, 1), \tag{5}$$

$$G_{yp}(\vec{U}^{(n)}, \vec{U}^{(n-1)}, \ldots) = R_{yp}\vec{U}^{(n)} + T_{,\vec{U}}(\vec{U}^{(n)} - \vec{U}^{(n-1)}) + T_{,\vec{U},x}(\vec{U}_{,x}^{(n)} - \vec{U}_{,x}^{(n-1)})$$

$$+ T_{,\vec{U},y}(\vec{U}_{,y}^{(n)} - \vec{U}_{,y}^{(n-1)}) + \vec{\varphi}_{yp} = 0, \quad y = y_p \quad (p = 0, 1), \tag{6}$$

where $D(\vec{U}^{(n)}, \vec{U}^{(n-1)}, \ldots)$, $G_{xp}(\vec{U}^{(n)}, \vec{U}^{(n-1)}, \ldots)$, $G_{yp}(\vec{U}^{(n)}, \vec{U}^{(n-1)}, \ldots)$ are differential or algebraic operators of the linearized problem containing the unknown functions of two successive approximations $\vec{U}^{(n)}$ and $\vec{U}^{(n-1)}$ and defined, respectively, in the given domain and on its boundary;

$$J_{,\vec{U},xy} = \left(\frac{\partial g_i}{\partial u_{j},xy} \right)\Bigg|_{\vec{U}=\vec{U}^{(n-1)}} \qquad (i, j = 1, 2, 3),$$

$$I_{,\xi} = \left(\frac{\partial s_{xpi}}{\partial u_{j},\xi} \right)\Bigg|_{\vec{U}=\vec{U}^{(n-1)}},$$

$$T_{,\xi} = \left(\frac{\partial s_{ypi}}{\partial u_{j},\xi} \right)\Bigg|_{\vec{U}=\vec{U}^{(n-1)}} \qquad (i = \overline{1,4},\ j = 1, 2, 3,\ \xi = 0,\ x,\ y).$$

Stage 2. The solution of a linearized problem from sequence (4)–(6) at each step of the quasilinearization (n = fixed) iteration using the MFIT*.

2.1. According to the main principles of this method [10], the original problem (4)–(6) is subject to the two integral transforms I and II with respect to different domain variables.

The integral transform I with respect to the variable $y \in [y_0, y_1]$ with kernel functions $\vec{Q}^{(n)} = \{q_{rk}^{(n)}(y)\}$, which are still unknown, is formulated in terms of transform functions

$$\vec{U}_x^{(n)} = \{r_\xi^{(n)}(x) = \int_{y_0}^{y_1} r^{(n)}(x,\ y)\ q_{ri}^{(n)}(y)\, dy\}$$

$$(r^{(n)} = u^{(n)},\ v^{(n)},\ w^{(n)}), \qquad (k = 1, 2, \ldots, K, \ldots)$$

and has the form

$$\int_{y_0}^{y_1} D(\vec{U}^{(n)}, \vec{U}^{(n-1)}, \ldots)\, q_{rk}^{(n)}(y)\, dy = 0, \qquad x \in (x_0,\ x_1),$$

$$\int_{y_0}^{y_1} G_{xp}(\vec{U}^{(n)}, \vec{U}^{(n-1)}, \ldots) q_{rk}^{(n)}(y)\, dy = 0, \qquad x = x_p \qquad (p = 0, 1). \tag{7}$$

When integrating Eq. (4) by parts, as in the classical method of finite integral transforms, the boundary conditions (6) for the integration variable y are taken into account.

The unknown solution of problem (4)–(6), which is the components of the displacement vector function $\vec{U}^{(n)} = \{r^{(n)}(x, y)\}\,(r^{(n)} = u^{(n)}, v^{(n)}, w^{(n)})$, is approximately determined using the inverse integral transform, which is a finite sum of the form

$$r^{(n)}(x, y) = F_{rK}^{(n)} \cong \sum_{i=1,\,2,\ldots K} r_\xi^{(n)}(x) q_{ri}^{(n)}(y). \tag{8}$$

Similarly, we obtain the integral transform II with respect to the variable $x \in [x_0, x_1]$ with kernel functions $\vec{P}^{(n)} = \{p_{rk}^{(n)}(x)\}$, which, as in the transform I, are unknown. It is formulated in terms of the transform functions

$$\vec{U}_y^{(n)} = \{r_{yi}^{(n)}(y) = \int_{x_0}^{x_1} r^{(n)}(x,\ y) p_{ri}^{(n)}(x) dx\}\,(r^{(n)} = u^{(n)}, v^{(n)}, w^{(n)})\,(k = 1, 2, \ldots, K, \ldots)$$

and has the following form:

$$\int_{x_0}^{x_1} D(\vec{U}^{(n)}, \vec{U}^{(n-1)}, \dots) p_{rk}^{(n)}(x)\, dx = 0, \qquad y \in (y_0, y_1),$$

$$\int_{x_0}^{x_1} G_{xp}(\vec{U}^{(n)}, \vec{U}^{(n-1)}, \dots) p_{rk}^{(n)}(x) dx = 0, \qquad y = y_p \quad (p = 0, 1). \tag{9}$$

The boundary conditions (5) for the transform variable x are taken into account.

The unknown solution of problem (4)–(6), which is $\vec{U}^{(n)} = \{r^{(n)}(x, y)\}$ $(r^{(n)} = u^{(n)}, v^{(n)}, w^{(n)})$, is approximately determined using the inverse integral transform

$$r^{(n)}(x, y) = S_{rK}^{(n)} \cong \sum_{i=1, 2, \dots K} r_{yi}^{(n)}(y) p_{ri}^{(n)}(x). \tag{10}$$

2.2. The kernels $\vec{Q}^{(n)} = \{q_{rk}^{(n)}(y)\}$ and $\vec{P}^{(n)} = \{p_{rk}^{(n)}(x)\}$ of the integral transforms I and II in the generalized method of finite integral transforms are fundamentally different from their classical variant [5, 7].

In the classical method of finite integral transforms (MFIT), the kernels are the eigenfunctions of the Sturm–Liouville problem. To find them, the operators of the original problem must meet the variable separation requirements, which significantly reduces the range of problems to which MFIT can be applied. The development of kernel functions of integral transforms that does not impose any additional restrictions on the statement of the problem is the major difference of the proposed generalization of these methods.

Thus, the MFIT* assumes that the kernel functions $\vec{Q}^{(n)} = \{q_{rk}^{(n)}(y)\}$ of the integral transform I are the transform functions $\vec{U}_y^{(n)} = \{r_{yi}^{(n)}(y)\}$ of the transform II, and the kernel functions $\vec{P}^{(n)} = \{p_{rk}^{(n)}(x)\}$ of the transform II are the transform functions $\vec{U}_x^{(n)} = \{r_{\xi}^{(n)}(x)\}$ of the transform I, i.e.:

$$q_{ri}^{(n)}(y) = r_{yi}^{(n)}(y), \qquad p_{ri}^{(n)}(x) = r_{\xi}^{(n)}(x),$$

$$(r^{(n)} = u^{(n)}, v^{(n)}, w^{(n)}) \qquad (i = 1, 2, \dots, K, \dots). \tag{11}$$

Under this condition, the expressions for the inverse transforms (8) and (10) are identical ($F_{rK}^{(n)} = S_{rK}^{(n)}$) and the unknown functions of problem (4)–(6) are defined as follows:

$$r^{(n)}(x, y) = F_{rK}^{(n)} \cong \sum_{i=1, 2, \dots K} r_{\xi}^{(n)}(x) r_{yi}^{(n)}(y). \tag{12}$$

Thus, with such a choice of kernel functions of integral transforms I and II, the solution of problems (4)–(6) is reduced to finding the functions $\vec{U}_x^{(n)} = \{r_{\xi}^{(n)}(x)\}$ and $\vec{U}_y^{(n)} = \{r_{yi}^{(n)}(y)\}$ from system (7), (9), which, taking into account (11), (12), and notation $\vec{F}^{(n)} = \{F_{rK}^{(n)} = S_{rK}^{(n)}\}$ $(r^{(n)} = u^{(n)}, v^{(n)}, w^{(n)})$, can be represented in the following form (arrows show the result of the corresponding integral transform):

$$\int_{y_0}^{y_1} D(F^{(n)}, F^{(n-1)}, \dots) r_{yk}^{(n)}(y) dy = 0 \to \tilde{L}_{(x)}^{(n-1)} \vec{U}_x^{(n)} + \tilde{\vec{f}}_{(x)}^{(n-1)} = 0, \qquad x \in (x_0, x_1);$$

$$\int_{y_0}^{y_1} G_{xp}(F^{(n)}, F^{(n-1)}, \dots) r_{yk}^{(n)}(y) dy = 0 \to \tilde{R}_{xp(x)}^{(n-1)} \vec{U}_x^{(n)} + \tilde{\vec{\varphi}}_{xp(x)}^{(n-1)} = 0, \qquad x = x_p \ (p = 0, 1); \tag{13}$$

$$\int_{x_0}^{x_1} D(F^{(n)},\, F^{(n-1)},\, \dots) r_{xk}^{(n)}(x)\,dx = 0 \to \widetilde{L}_{(y)}^{(n-1)} \vec{U}_y^{(n)} + \vec{\tilde{f}}_{(y)}^{(n-1)} = 0, \qquad y \in (y_0, y_1);$$

$$\int_{x_0}^{x_1} G_{yp}(F^{(n)},\, F^{(n-1)},\, \dots) r_{xk}^{(n)}(x)\,dx = 0 \to \widetilde{R}_{yp(y)}^{(n-1)} \vec{U}_y^{(n)} + \vec{\tilde{\varphi}}_{yp(y)}^{(n-1)} = 0, \qquad y = y_p \ (p = 0, 1). \tag{14}$$

This new structure is a system of two integral transforms of the linearized problem (4)–(6), which corresponds to two conditionally one-dimensional problems (13) and (14) for different domain variables (expressions after arrows $\to$).

Thus, problem (13) (expressions after arrows $\to$) is stated with respect to the functions $\vec{U}_x^{(n)} = \{r_\xi^{(n)}(x)\}$ ($r^{(n)} = u^{(n)}, v^{(n)}, w^{(n)}$) of the variable x, "~" denotes the linear operators of the linearized problem $\widetilde{L}_{(x)}^{(n-1)}$, $\widetilde{R}_{xp(x)}^{(n-1)}$ and the vector functions of its free terms $\vec{\tilde{f}}_{(x)}^{(n-1)}$ and $\vec{\tilde{\varphi}}_{xp(x)}^{(n-1)}$: the superscript $(n-1)$ means that they depend on the functions $\vec{U}_x^{(n-1)} = \{r_\xi^{(n-1)}(x)\}$ of the previous step of linearization, the subscript in parentheses (x) indicates that the operators and vectors are obtained according to the integral transform I and, due to (12), contain unknown functions $\vec{U}_y^{(n)} = \{r_{yi}^{(n)}(y)\}$ of the variable y in the form of functional constants.

Similarly, problem (14) (expressions after arrows $\to$) is stated with respect to the functions $\vec{U}_y^{(n)} = \{r_{yi}^{(n)}(y)\}$ ($r^{(n)} = u^{(n)}, v^{(n)}, w^{(n)}$) of the variable y, "~" also denotes the linear operators of the linearized problem $\widetilde{L}_{(y)}^{(n-1)}$, $\widetilde{R}_{yp(y)}^{(n-1)}$ and the vector functions of its free terms $\vec{\tilde{f}}_{(y)}^{(n-1)}$ and $\vec{\tilde{\varphi}}_{yp(y)}^{(n-1)}$: the superscript $(n-1)$ means that they depend on the functions $\vec{U}_y^{(n-1)} = \{r_{yi}^{(n-1)}(y)\}$ of the previous linearization step, the subscript in parentheses (y) means that the operators and vectors are obtained according to the integral transform II and, due to (12), contain unknown functions $\vec{U}_x^{(n)} = \{r_\xi^{(n)}(x)\}$ of the variable x in the form of functional constants.

To solve the system of one-dimensional problems (13), (14) to find the kernel functions $\vec{U}_x^{(n)} = \{r_\xi^{(n)}(x)\}$ and $\vec{U}_y^{(n)} = \{r_{yi}^{(n)}(y)\}$, the Liebmann–Gauss–Seidel process is used as an analogue of the method of successive substitutions in linear algebra. Its iteration scheme is as follows (iteration parameter j):

$$\widetilde{L}_{(x)}^{(n-1)(j-1)} \vec{U}_x^{(n)(j)} + \vec{\tilde{f}}_{(x)}^{(n-1)(j-1)} = 0, \qquad x \in (x_0, x_1);$$

$$\widetilde{R}_{xp(x)}^{(n-1)(j-1)} \vec{U}_x^{(n)(j)} + \vec{\tilde{\varphi}}_{xp(x)}^{(n-1)(j-1)} = 0, \qquad x = x_p \quad (p = 0, 1); \tag{15}$$

$$\widetilde{L}_{(y)}^{(n-1)(j)} \vec{U}_y^{(n)(j)} + \vec{\tilde{f}}_{(y)}^{(n-1)(j)} = 0, \qquad y \in (y_0, y_1);$$

$$\widetilde{R}_{yp(y)}^{(n-1)(j)} \vec{U}_y^{(n)(j)} + \vec{\tilde{\varphi}}_{yp(y)}^{(n-1)(j)} = 0, \qquad y = y_p \quad (p = 0, 1) \tag{16}$$

(the superscripts in parentheses indicate the parameters of two different iterative processes: linearization (n) and the Liebmann–Gauss–Seidel (j)).

Thus, the kernel functions $\vec{U}_x^{(n)(j)}$, $\vec{U}_y^{(n)(j)}$ of two integral transforms with respect to different domain variables are determined in two iterative processes: the external process of linearization (parameter n) and the internal Liebman–Gauss–Seidel process of solving the system of one-dimensional problems (parameter j).

Stage 3. To solve the nonlinear problem (4)–(6) in this class of problems of the theory of shells, it is possible to develop a joint iterative process that combines both of the above types of iterations: linearization of the original problem (parameter n) and the Liebmann–Gauss–Seidel solution of the system of one-dimensional problems (parameter j):

$$\widetilde{L}_{(x)}^{(m-1)}\vec{U}_x^{(m)} + \widetilde{\vec{f}}_{(x)}^{(m-1)} = 0, \quad x \in (x_0, x_1);$$

$$\widetilde{R}_{xp(x)}^{(m-1)}\vec{U}_x^{(m)} + \widetilde{\vec{\varphi}}_{xp(x)}^{(m-1)} = 0, \quad x = x_p \quad (p = 0, 1); \tag{17}$$

$$\widetilde{L}_{(y)}^{(m-1)}\vec{U}_y^{(m)} + \widetilde{\vec{f}}_{(y)}^{(m-1)} = 0, \quad y \in (y_0, y_1);$$

$$\widetilde{R}_{yp(y)}^{(m-1)}\vec{U}_y^{(m)} + \widetilde{\vec{\varphi}}_{yp(y)}^{(m-1)} = 0, \quad y = y_p \quad (p = 0, 1) \tag{18}$$

($m = 1, 2, \ldots$ is the joint process parameter).

The initial approximation for this joint iteration can be chosen as follows: the zero vector $\vec{U}_x^{(0)} = \{r_\xi^{(0)}(x\} \equiv \vec{0}$ is chosen as the vector function $\vec{U}_x^{(0)}$, and any linearly independent (in i) functions (trigonometric, power, polynomial, etc.) are chosen for the components of the vector function $\vec{U}_y^{(0)} = \{r_{yi}^{(0)}(y)\}$. Then the one-dimensional problem (17) in the first approximation corresponds to the linear statement of the original problem.

Further, the system of one-dimensional problems (17)–(18) of finding the kernel functions $\vec{U}_x^{(m)}$, $\vec{U}_y^{(m)}$ at the intermediate mth step of the approximation is solved as follows:

– calculation of the coefficients of operators and vector functions of free terms of problem (17), using the values of the vector function $\vec{U}_x^{(m-1)}$ and $\vec{U}_y^{(m-1)}$ from the previous $(m-1)$ step of the joint process;

– finding of the solution $\vec{U}_x^{(m)}$ of the one-dimensional problem (17) using the orthogonal sweep method;

– calculation of the coefficients of the operators and vector functions of free terms of problem (18), using the solution $\vec{U}_x^{(m)}$ and the vector $\vec{U}_y^{(m-1)}$ known from the previous approximation;

– finding of the solution $\vec{U}_y^{(m)}$ of the one-dimensional problem (18) using the orthogonal sweep method;

– checking of the accuracy of the kernel functions $\vec{U}_x^{(m)}, \vec{U}_y^{(m)}$ against the chosen criterion; if the specified accuracy is achieved, finding of the unknown displacement vector $\vec{U}^{(m)}$ using the inverse integral transform (12), or, otherwise, moving to the next $(m+1)$-approximation.

The iterative process of solving system (17), (18) with a fixed number K of terms in (12) is terminated if the following well-known criterion of applied mathematics is met:

$$\left|1 - \frac{\gamma^{(m)}}{\gamma^{(m-1)}}\right| \le \varepsilon_1,$$

where $\gamma^{(m)} = \max\{\gamma_{q^{(m)}}^{(m)}\}$ $(q^{(m)} = u^{(m)}, v^{(m)}, w^m)$, $\gamma_{q^{(m)}}^{(m)}$ is the maximum or root mean square value of the function $F_{rK}^{(m)}$ in the inverse transform (12); ε_1 is the specified accuracy of the kernel functions $\vec{U}_x^{(m)}, \vec{U}_y^{(m)}$.

The accuracy ε_2 of the final solution of problem (4)–(6) is achieved by keeping a larger number K of terms in (12). It is controlled using a similar criterion:

$$\left|1 - \frac{\gamma^{(K)}}{\gamma^{(K-1)}}\right| \le \varepsilon_2.$$

3. Practical Substantiation of the Developed Approach. Unfortunately, the numerical analytical approach to solving nonlinear boundary-value problems based on the generalized method of finite integral transforms and the quasilinearization method does not have a strictly theoretical substantiation. Therefore, as in the linear case [10, 11], we use only individual examples of its practical substantiation, which is important for applied research. Such substantiation is carried out inductively, in particular by comparing with the results obtained by other methods.

TABLE 1

m ↓	$\zeta = w_{\max} / h$			
	K			[4]; ε,%
	1	2	3	
1	3.115	1.933	2.003	1.94; 1.8%
2	2.512	2.014	1.948	
3	2.407	1.975	1.975	
4	2.268	**1.975**	**1.975**	
5	1.807			
6	1.807			

TABLE 2

m ↓	K				[4], ε,%
	1	2	3	4	
1	1.433	1.452	1.480	1.486	
2	2.071	1.509	1.482	1.473	
3	1.825	1.510	1.517	1.518	**1.50**
4	1.551	1.518	1.518	1.518	
5	1.474	1.518	1.518		1.2%
6	1.462	1.518			
7	1.462				

Based on the developed approach, the following procedures are to be tested:

– the convergence of the joint process of solving the system of integral transforms to determine a fixed number K of unknown kernel functions, which combines the Newton–Kantorovich–Raphson linearization and the Liebmann–Gauss–Seidel solution of a separate linearized problem (process (17), (18), K = fixed);

– convergence of the final solution of the problem with a greater number K of kernel functions kept in the inverse integral transform (12) $K = 1, 2, \ldots, (K+1)$.

Examples from [4, 20] are included to demonstrate the satisfaction of these conditions.

Problem 1. Consider a shallow isotropic panel of constant thickness h that occupies a domain $a \times b$ in plan and has curvatures k_x and k_y along the coordinate axes Ox and Oy, respectively. The shell is hinged along the entire edge and is under a uniformly distributed normal load of intensity $q_n(x, y) = q$, which is directed toward the center of curvature. The curvature of the panel and the effective load are described, as in [4], by dimensionless parameters $k_x^* = k_x b^2 / h$, $k_y^* = k_y b^2 / h$, $q^* = qb^4 / (Eh^4)$ (E is Young's modulus).

TABLE 3

q^* ↓	K			[4]	ε, %
	1	3	4		
15.92	0.491	0.490	0.490	**0.490**	0.0
23.95	0.993	1.010	1.010	**1.00**	1.0
44.51	1.971	2.011	2.011	**1.99**	1.00
70.56	2.481	2.530	2.530	**2.48**	2.02
115.6	2.950	3.060	3.060	**2.95**	3.72

TABLE 4

k_x^*, k_y^*	q_-^*	q_+^*	$q_{cr}^* \in [q_-^*, q_+^*]$	[4] (ε,%)
0; 20	44.75	44.76	[44.75; 44.76]	44.81 (0.13)
15; 15	97.99	98.00	[97.99; 98.00]	105.70 (7.3)
25;25	377.55	377.56	[377.55; 377.56]	395.53 (4.5)

Using this shell as an example, we show the convergence of the joint iteration (17), (18) depending on the iteration step m for different number K of kernel functions of the inverse transform (12). These data for the dimensionless maximum deflection $\zeta = w_{\max} / h$ are given in Table 1 for cylindrical panel with a rectangular planform with ratio of side lengths $\lambda = b / a = 2/3$, curvature $k_y^* = 10$ when $q^* = 25, 53$, in Table 2 for the spherical panel with a square planform with curvatures $k_x^* = k_y^* = 6$ and $q^* = 31.17$, and in Table 3 depending on the number K of kernel functions in (12) for the same spherical panel. The last columns of the tables contain the data from [4] obtained by the Ritz variation method in three approximations, and the relative difference between the results $\varepsilon = (|\zeta_{[4]} - \zeta_{(\text{appr})}| / \zeta_{[4]}) \cdot 100$.

The input data: $\lambda = b / a = 1, 2/3$, $b = 0.1$ m, $h = 10^{-3}$ m, $E = 9.81 \cdot 10^{10}$ N/m^2, $\mu = 0.3$.

The data (Tables 1, 2, 3) shows that the joint iterative process of solving the original nonlinear problem converges quite quickly (m = 5–7) for the given values of K in the inverse transform (12) and has a constant value when $K = 2$ or when $K = 3$. The difference of results (last columns in Table 1–3) is within 3–4%.

Let us determine the critical load q_{cr} under which the panel "snaps" (snap-through buckling).

Note that the quasilinearization method automatically reduces the domain of its application to subcritical deformation, so that the joint iterative process (17), (18) converges only in this domain. This fact, as shown in [3], can be used to approximately determine the upper critical load q_{cr} according to the following criterion: $q_{cr} \in [q_-, q_+)$, where q_- is the load under which the iterative procedure (17), (18) still converges, and q_+ is the load under which this process diverges. Thus, q_- and q_+ are the computational limits of the unknown critical load. These data for shells of different curvatures and for different load values are given in Table 4 and compared with the results of [4].

The table shows that the difference between the critical values obtained by the developed approach and in [4] is within 8%.

Problem 2. Consider an isotropic cylindrical panel $a \times a$ with a square planform of constant thickness h with rise f_x under uniform external pressure q. The arc edges of the panel are free from loads ($y = 0, a$: $T_2 = S = Q_2 = M_2 = 0$), and the straight edges are rigidly hinged ($x = 0, a$: $u = v = w = M_1 = 0$) [20].

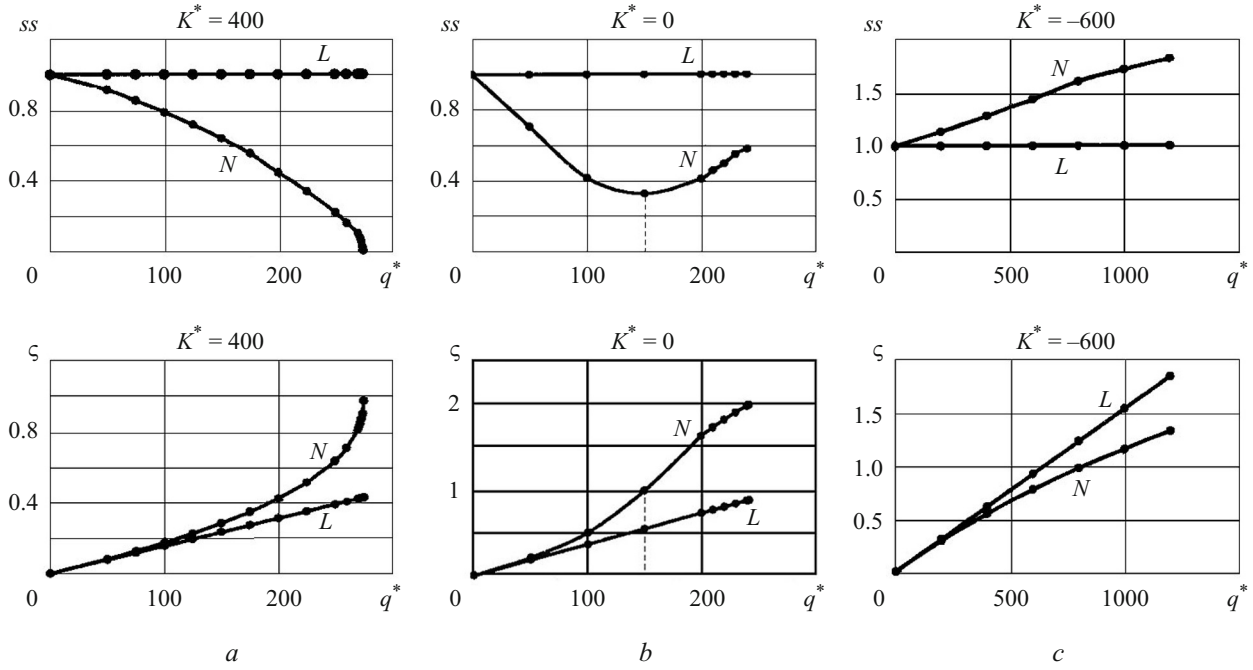

Fig. 1

According to the computational criterion outlined in the last example of the previous problem ($q_{cr} \in [q_-, q_+)$, where q_-, q_+ are the values of the loads under which the iterative process (17), (18) converges and diverges, respectively), the critical pressure q_{cr} under which the panel snaps through is determined.

The results are presented for the following input data [20]:

$$a = 2 \text{ m}, \quad f_x = 0.1 \text{ m}, \quad h = 0.02 \text{ m}, \quad E = 210 \text{ GPa}, \quad \mu = 0.3.$$

The calculated values are $q_- = 0.5683$ N/mm^2, $q_+ = 0.5684$ N/mm^2. Thus the unknown critical value is within the following boundaries: $0.5683 \le q_{cr} < 0.5684$ [N/mm^2].

In [20], this problem was solved using the FEM (ANSYS application) and it was found that $q_{cr} = 0.576$ N/mm^2.

Thus, the difference between the critical pressure values obtained using the FEM and the proposed approach does not exceed 1.5%.

The above examples improve the reliability of the approach for the class of nonlinear problems of the theory of shallow shells.

4. Nonlinear Deformation of Shells. Let us analyze the dependence of the nonlinear strain of the shallow shell (panels) described above on the following factors:

– Gaussian curvature of different signs over a wide range of changes in its values;

– combinations of clamped and free edges of the panel;

– discrete inclusions with different locations.

Consider an isotropic (E, μ) panel of constant thickness h with square planform ($a \times a$) and curvatures k_x, k_y along the coordinate axes $0x$ and $0y$ under a uniform external load of intensity $q_n(x, y) = q_0$. As before, we will describe the deflection of the panel, its curvature, load intensity, and axis coordinates using the following dimensionless parameters: $\varsigma = w_{\max} / h$; $k_x^* = k_x a^2 / h$; $k_y^* = k_y a^2 / h$; $K^* = k_x^* k_y^*$; $q^* = (q_0 a^4) / (Eh^4)$; $\tilde{x} = x / a$; $\tilde{y} = y / a$.

In the first part, we analyze the effect of the load q^* on the static stiffness of the panel in the vicinity of its largest deflection $ss = (dq^* / d\varsigma) / ss(0)$ and on the traditional load–deflection relationship $\varsigma = \varsigma(q^*)$ ($ss(0)$ is the stiffness of the shell without load). Figure 1 shows these data for $ss = ss(q^*)$ (left column) and for $\varsigma = \varsigma(q^*)$ (right column) for constant curvature $k_x^* = 20$ and different values of curvature $k_y^* \in [20, -30]$, so that the Gaussian curvature covers a wide range of positive, negative, and zero values $K^* \in [400, -600]$ (Fig. 1 shows the dependences for $K^* = 400, K^* = 0, K^* = -600$).

In the considered range of curvatures $K^* \in [400, -600]$, the dependences $ss = ss(q^*)$ and $\varsigma = \varsigma(q^*)$ have obvious qualitative differences of which three types are characteristic:

(a) panels of positive Gaussian curvature $k_y^* = 20$, $K^* = 400$, $q_{cr}^* = 275$ (Fig. 1*a*): during nonlinear deformation (notation *N* in the figure), $ss = ss(q^*)$ monotonically decreases to zero under critical load $q_{cr}^* = 275$ and so does $\varsigma = \varsigma(q^*)$, and the snap-through buckling of the panel can be expected;

(b) panels of zero curvature $k_y^* = 0$, $K^* = 0$ (Fig. 1*b*); it is hard to predict their behavior with increasing load and their static stiffness in the nonlinear case is represented by a nonmonotonic function $ss = ss(q^*)$ with minimum point $q^* = 150$ at which the behavior of this curve changes; the curve $\varsigma = \varsigma(q^*)$ has an inflection at this point;

(c) panels of negative Gaussian curvature $k_y^* = -30$, $K^* = -600$ (Fig. 1*c*): their static stiffness $ss = ss(q^*)$ is a monotonically increasing function for all subcritical load values from the considered range; the curve $\varsigma = \varsigma(q^*)$ is located below its linear case (*L*) and such shells are not prone to snap-through buckling with increasing load.

It is quite natural that for all types of curvatures the static stiffness does not change in the linear case (*L*).

Thus, the analysis for the simple example of a square panel clamped along the edge illustrates the ambiguous effect of the Gaussian curvature of shells on their stability.

In the second part, we consider various boundary conditions for flexible shells undergoing nonlinear deformation.

Note that the analysis of the stability of shallow panels was and is usually restricted to combinations of hinged and clamped edges [6, 9, 25]. When constructing various buildings such as industrial facilities, railway stations, hangars, etc., individual sections of shallow roof or floor panels must be free from any restrictions according to architectural requirements (corner ledges, rectangular ledges with one free edge, canopies, etc.). This necessitates studying all aspects of stationary deformation (SSS, vibrations, stability) for a combination of different boundary conditions, including a free edge. There are few works on the stability of shallow shells (for example, [20]).

Since further studies are related to the analysis of the stability of a shallow panel with clamped and free edges.

Consider a spherical panel with curvatures $k_x^* = k_y^* = 20$ depending on the parameter $\xi = lf / ll$ (ratio of the length of the unloaded section of the boundary (*lf*) to the length of the entire boundary (*ll*)). The following four cases of boundary conditions are considered:

$n = 1$: $\xi = 0$ (all edges of the panel are clamped);

$n = 2$: $\xi = 1/4$ (one edge is free, the others are clamped);

$n = 3$: $\xi = 1/2$ (two adjacent edges are free, the other two are clamped);

$n = 4$: $\xi = 3/4$ (three edges are free, one is clamped (console)).

In the cases $n = 1 \div 4$, the free edge certainly affects the behavior of static stiffness $ss = ss(q^*)$ and the load–deflection relationship $\varsigma = \varsigma(q^*)$, but there are no qualitatively new cases compared with those in Fig. 1. By their nature, the relationships for $n = 1$ and $n = 2$ ($\xi = 0$, $\xi = 1/4$) correspond to those in Fig. 1*a*, that is, the panel can snap with increasing load. The other two cases $n = 3$ and $n = 4$, where the free edge is larger ($\xi = 1/2$, $\xi = 3/4$), are characterized by an increase in static stiffness, and these panels are not expected to snap with increasing pressure (similar cases are presented in Fig. 1*c*).

In the third part, the two previous problems are somewhat complicated. The complication is, in particular, due to the fact that broad aspects of the application of shallow shells assumed the use of reinforcing ribs, pads, elastic (rigid) supports, etc. These features introduce structural inhomogeneity into the model, which greatly complicates the determination of the critical load and the assessment of the bearing capacity of the object. Thus, there is a need for rational selection of discrete inclusions: arrangement, stiffness, localization on the panel, etc. This mainly applies to panels with a part of the edge free from load. Such shells are used as an example to analyze the critical normal pressure depending on the arrangement of discrete inclusions.

A discrete inclusion is described using the Winkler foundation model with Winkler coefficient

$$K_p(x, y) = \begin{cases} c_0, & (x, y) \in \Omega_0, \\ 0, & (x, y) \notin \Omega_0, \end{cases}$$

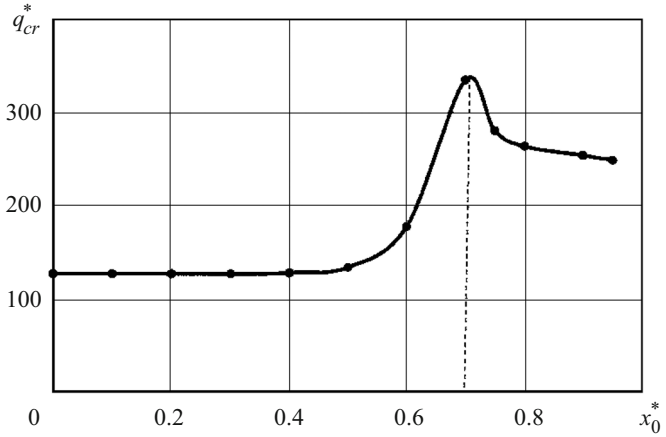

Fig. 2

where c_0 is the stiffness of the inclusion; $\Omega_0 = \{x, y: |x - x_0| \le r_x, |y - y_0| \le r_y\}$ is a rectangular domain with area $2r_x \times 2r_y$ centered at the point O with coordinates $x = x_0$, $y = y_0$. The localization of the inclusion in the domain Ω is described by the dimensionless parameter $\eta = \Omega_0 / \Omega$; its relative stiffness $\tilde{c} = c_0 / (9.8 \cdot 10^9)$, the location of the inclusion is determined by the position of its center $O^*(x_0^*, y_0^*)$ $(x_0^* = x_0 / a, y_0^* = y_0 / a)$.

For a square spherical panel with curvatures $k_x^* = k_y^* = 20$ and one free edge $\tilde{x} = 1$ $(\xi = 1/4)$ and three clamped edges $(\tilde{x} = 0, \tilde{y} = 0, \tilde{y} = 1)$, we study the effect of the position of a discrete inclusion on the stability of the panel in the form of the function $q_{cr}^* = q_{cr}^*(0^*)$.

We consider the case where the support inclusion is placed in the cross-section $y_0 = a/2$ $(y_0^* = 0.5)$ (the panel is symmetric about the coordinate y), and its position is determined by the coordinate $x_0^* \in (0, 0.95]$ only. The dependence of the critical external pressure $q_{cr}^* = q_{cr}^*(x_0^*)$ is presented in Fig. 2 for $\eta = 0.01$. This curve, contrary to expectations, is nonmonotonic with the highest critical load when the support is in the vicinity of the point $x_0^* \simeq 0.7$. For the range $x_0^* \in (0, 0.4]$, the inclusion has a weak effect on the critical value q_{cr}^*: here the clamping of the edges $\tilde{x} = 0$, $\tilde{y} = 0$, $\tilde{y} = 1$ plays a decisive role, which practically negates the effect of the support. In terms of panel stability, the position of the support in the immediate vicinity of the boundary of the domain $x_0^* \simeq 0.95$ turned out not to be optimal. When the support is in this position, the critical pressure q_{cr}^* is less by 25% than its maximum value at $x_0^* \simeq 0.7$.

Figure 3 demonstrates the effect of the position of the discrete inclusion on the pattern of deflections of the panel midsurface. The figure shows the distribution of displacements $\varsigma = \varsigma(\tilde{x})$ over the central cross-section $\tilde{y} = 0.5$ for different locations of the inclusion $x_0^* \simeq 0, 0.4, 0.7, 0.95$ under load q^* close to the critical one: $q^* = 120$ $(x_0^* = 0, x_0^* = 0.4)$; $q^* = 330$ $(x_0^* = 0.7)$; $q^* = 254$ $(x_0^* = 0.95)$ (Fig. 3*a*).

Figure 3*b* shows the distribution of displacements $\varsigma = \varsigma(\tilde{y})$ over the cross-section $\tilde{x} = 0.5$ for the same locations of the inclusion x_0^* under the same loads q^*.

This study of the nonlinear deformation of shallow panels demonstrated the dependence of their stability on the values and signs of Gaussian curvatures, various combinations of clamped and load-free sections of the boundary, and the location of discrete inclusions.

Conclusions. We have proposed a numerical analytical approach to the study of the nonlinear deformation of shallow shells under subcritical loads, based on a rational combination of the generalized method of finite integral transforms and the Newton–Kantorovich–Raphson linearization method.

We have considered some examples of practical substantiation of the developed approach that improve the reliability of the results obtained in the class of nonlinear problems of the theory of shallow shells.

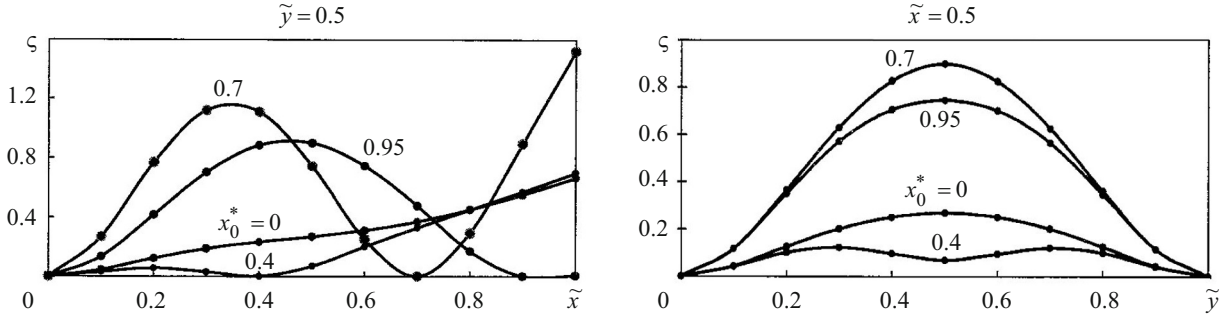

a *b*

Fig. 3

We have analyzed the static stiffness and the load–deflection relationship of discretely inhomogeneous flexible shallow shells over a wide range of change in their Gaussian curvature under various boundary conditions, including the presence of a free edge.

For a clamped shell, three ranges of Gaussian curvature values for which the panel under an external load: (a) can undergo snap-through buckling; (b) displays ambiguous behavior with increasing load; (c) is not prone to buckling.

The effect of the location of a solid inclusion on the stability of the panel with three clamped sections of the edge and one free section has been studied. It has been shown that the dependence of the critical external pressure on the location of inclusions is usually a nonmonotonic function. This makes it possible to determine their optimal location in terms of panel stability and bearing capacity.

REFERENCES

1. V. A. Bazhenov, N. A. Solovei, and O. P. Krivenko, "Stability of shallow shells of revolution with linearly variable thickness," *Aviats.-Kom. Tekhn. Tekhnol.*, **10**, No. 2, 18–25 (2004).
2. R. E. Bellman and R. E. Kalaba, *Quasilinearization and Nonlinear Boundary-Value Problems*, Elsevier, New York (1965).
3. Ya. M. Grigorenko, E. I. Bespalova, A. B. Kitaigorodskii, and A. I. Shinkar', "Numerical solution of nonlinear boundary-value problems of the statics of flexible shells," *Dokl. AN USSR, Ser. A*, No. 6, 44–48 (1986).
4. M. S. Kornishin, *Nonlinear Problems in the Theory of Plates and Shallow Shells and Methods to Solve Them* [in Russian] Nauka, Moscow (1964).
5. N. S. Koshliakov, E. B. Gliner, and M. M. Smirnov, *Main Differential Equations of Mathematical Physics* [in Russian], Fizmatgiz, Moscow (1962).
6. O. P. Kryvenko, "The effect of heating on the stability and natural vibrations of a spherical panel upon changes in the combined boundary conditions," *Opir Mat. Teor. Sporud*, No. 96, 48–64 (2015).
7. Yu. E. Senitskii, "Finite integral transform method: Generalization of the classical procedure of expansion into series of vector eigenfunctions," *Izv. Saratov. Univ., Ser. Mat. Mekh. Inform.*, No. 3 (1), 61–89 (2011).
8. M. Amabili, "Nonlinear vibrations and stability of doubly curved shallow-shells: isotropic and laminated materials," in: *Nonlinear Vibrations and Stability of Shells and Plates*, Cambridge University Press (2008), pp. 272–297.
9. J. Awrejcewicz, L. Kurpa, and T. Shmatko, "Analysis of geometrically nonlinear vibrations of functionally graded shallow shells of a complex shape," *Lat. Am. J. Solids Struct.*, **9**, No. 14, 1648–1668 (2017).
10. E. I. Bespalova, "On the method of finite integral transforms in problems of statics of inhomogeneous plates," *Int. Appl. Mech.*, **50**, No. 6, 651–663 (2014).
11. E. I. Bespalova, "Generalized method of finite integral transforms in static problems for anisotropic prisms," *Int. Appl. Mech.*, **54**, No. 1, 41–55 (2018).
12. E. Bespalova and G. Urusova, "Solution of the lame problem by the complete systems method," *Int. J. for Comp. Meth. Eng. Sci. Mech.*, **14**, No. 2, 159–167 (2013).

13. D. H. Campen, V. P. Bouwman, G. Q. Zhang, J. Zhang, and B. J. W. Weeme, "Semi-analytical stability analysis of doubly-curved orthotropic shallow panels-considering the effects of boundary conditions," *Int. J. of Non-Lin. Mech.*, **37**, No. 4–5, 659–667 (2002).
14. N. D. Duc and T. Q. Quan, "Nonlinear stability analysis of double-curved shallow fgm panels on elastic foundations in thermal environments," *Mech. Comp. Mater.*, **48**, No. 4, 435–448 (2012).
15. A. Garg, H. D. Chalak, M. O. Belarbi, A. M. Zenkour, and R. Sahoo, "Estimation of carbon nanotubes and their applications as reinforcing composite materials – an engineering review," *Comp. Struct.*, No. 272, 114234 (2021).
16. Ya. M. Grygorenko and L. S. Rozhok, "Analysis of stress state of hollow orthotropic cylinders with oval cross-section," *Int. Appl. Mech.*, **57**, No. 2, 45–57 (2021).
17. S. Huang and P. Qiao, "A new semi-analytical method for nonlinear stability analysis of stiffened laminated composite doubly-curved shallow shells," *Comp. Struct.*, **251**, No. 1.112526 (2020).
18. R. Kumar, L. S. Ramachandra, and B. Banerjee, "Nonlinear stability characteristics of composite cylindrical panel subjected to non-uniform in-plane mechanical and localized thermal loadings," *Proc. Ind. Nat. Sci. Acad.*, **82**, No. 2, 271–288 (2016).
19. S. Kurukuri, "Stability and geometrical nonlinear analysis of shallow shell structures," *Adv. Mech. of Mat. and Struct. Grad. School of Struct. Eng. Project-2*, Bauhaus Universität, Weimar, 1–46 (2004).
20. M. Psotny and J. Havran, "Stability analysis of an open shallow cylindrical shell with imperfection under external pressure," in: *MATEC Web of Conferences*, Slovak University of Technology, Bratislava (2017), pp. 1–6.
21. D. P. Roberts, "Numerical modelling of blocky and stratified hangingwall behaviour," in: *6-th Int. Symposium on Ground Support in Mining and Civil Engineering Construction, SAIMM, SANIRE and ISRM* (2008), pp. 329–344.
22. N. P. Semenyuk and N. B. Zhukova, "Stability of a sandwich cylindrical shell with core subject to external pressure and pressure in the inner cylinder," *Int. Appl. Mech.*, **56**, No. 1, 40–53 (2020).
23. N. P. Semenyuk and N. B. Zhukova, "Effect of mechanical and geometric parameters of composite cylindrical shells with localized deflection on character of equilibrium curves under axial compression," *Int. Appl. Mech.*, **57**, No. 1, 75–87 (2021).
24. B. P. Watson and R. Gerber, "Determination of stable spans in UG2 excavations," *J. of the South. Afric. Inst. of Min. and Met.*, **118**, No. 5, 493–504 (2018).
25. J. Z. Zhang and D. H. van Campen, "Stability and bifurcation of doubly curved shallow panels under quasi-static uniform load," *Int. J. of Non-Lin. Mech.*, **38**, No. 4, 457–466 (2003).